Semi-Classical Investigation of the Efimov Potential in Small Nuclei

Edward Sutherland, Cyclotron Institute, Texas A&M University
(REU student from Hillsdale College)
Advisor: Dr. Aldo Bonasera

Introduction

Various theories exist to explain the disagreement between the energy predicted by classical models of nuclei and established experimental values of the energy. One such theory that has had some verification in a quantum model when extended to atomic systems [3] was introduced by Vitaly Efimov and is known as the Efimov potential. However, each of the successes of the Efimov potential in predicting small systems of particles comes with pairing the Efimov potential to a complex quantum mechanical model. A semi-classical model and understanding of the Efimov potential has not been reached.

Purpose

The primary purpose of this research is to attempt to model small nuclei by pairing the Efimov potential with a semi-classical system. The secondary purpose is to explore the causes and ramifications of the pairing and to attempt to locate the Efimov states.

Methods

We used the Yukawa potential for the majority of our investigation with a kinetic energy factor

$$KE = \frac{P^2}{2m}$$

such that $rP=\hbar$. Our Efimov potential was derived from the work of Braatan and Hammer [4] to satisfy

$$E_{r\to\infty}(r) = \frac{-2(1+s_0^2)\hbar^2}{3m\,R^2} \quad \text{where} \quad R^2 = \frac{2}{9}\left(r_{ab}^2 + r_{bc}^2 + r_{ca}^2\right)$$

We used two different geometric models each with a slightly different Efimov potential to investigate the three particle nuclei. One, Model A, [See Fig. 1] was an equilateral triangle model with relative momentum (P) between nucleons. The second model, Model B, was an isosceles triangle with side lengths *r, r, and r/2* respectively, and momenta assigned to each particle to satisfy the uncertainty principle $rP=\hbar$ [See Fig. 1].

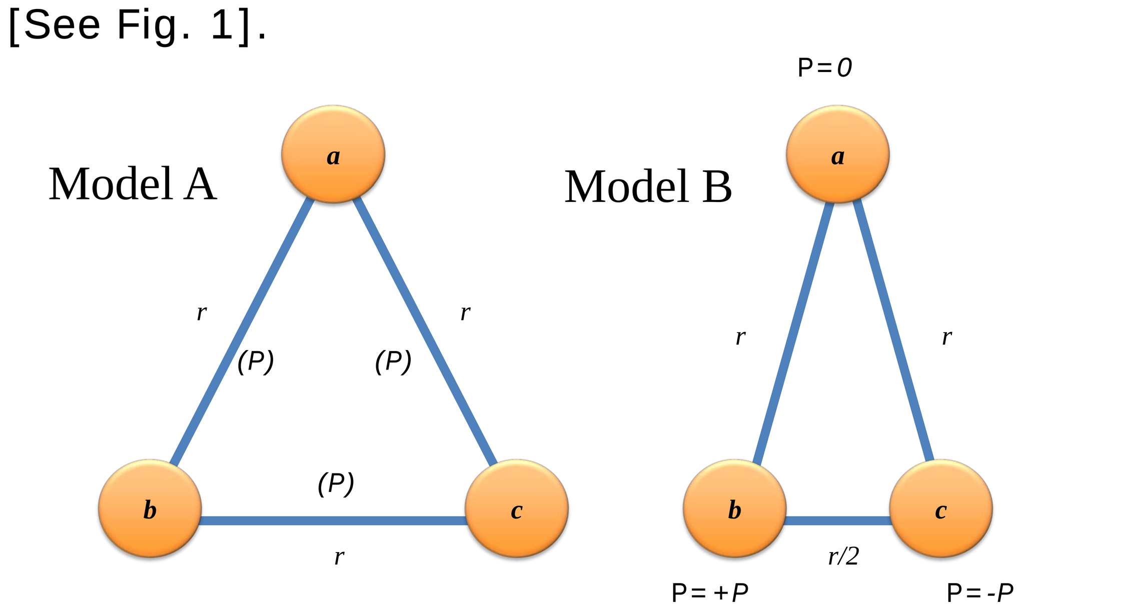

Fig. 1. Models A and B with respective momenta and radii.

First, the kinetic energy model was confirmed by using the model to calculate the energy of known systems, H, He_2, and Li_3. For H and He_2 the model gave energies and radii that matched confirmed experimental measurements. For Li_3 the model differed slightly but variance was attributed to its non-bosonic nature.

With the kinetic factor confirmed the model was applied to an idealized three nucleon system of identical particles in both geometrical configurations discussed earlier. The two-body conditions of the system were $E(r_d) = 0$ and $E'(r_d) = 0$, where

$$E(r_d) = KE + V_{Yukawa}(r_d)$$

or

$$E(r_d) = \frac{c_a\, e^{-r_d \mu_a}}{r_d} + \frac{c_r\, e^{-r_d \mu_r}}{r_d} + \frac{\hbar^2}{4m{r_d}^2}$$

In this equation r_d is the two body radius, μ_a is the pion attractive parameter, and μ_r is the pion repulsive parameter.

After choosing a radius r_d and solving for the parameters c_a and c_r the results were used to calculate the energy of the two models

$$E_A(r_t) = 3\left(\frac{c_a\, e^{-r_t \mu_a}}{r_t} + \frac{c_r\, e^{-r_t \mu_r}}{r_t}\right) + \left(\frac{3\hbar^2}{m{r_t}^2}\right) - \left(\frac{(4+{s_0}^2)\hbar^2}{m{r_t}^2}\right)$$

$$E_B(r_t) = 2\left(\frac{c_a\, e^{-r_t \mu_a}}{r_t} + \frac{c_r\, e^{-r_t \mu_r}}{r_t}\right) + \left(\frac{c_a\, e^{-\left(\frac{r_t}{2}\right)\mu_a}}{\left(\frac{r_t}{2}\right)} + \frac{c_r\, e^{-\left(\frac{r_t}{2}\right)\mu_r}}{\left(\frac{r_t}{2}\right)}\right) + \left(\frac{3\hbar^2}{m{r_t}^2}\right) - \left(\frac{(4+{s_0}^2)\hbar^2}{m{r_t}^2}\right)$$

With reasonable results from the ideal model, both geometric models A and B were then applied to three different cases of triton with the modification of a proton replacing the particle at position ***a*** [See Fig. 1]. (The proton was placed at the apex of the triangle because it minimized distortion of the deuteron-like bond.) In Case I, identical to the idealized case, parameters c_a and c_r were calculated for a two nucleon interaction where $E(r_d)=0$ and $E'(r_d)=0$. In Case II, the scattering length of the two nucleon interaction was set at 23.71*fm* and the parameters were recalculated. In Case III, $E'(r_d)=0$ and $E''(r_d)=0$ and once again the parameters were recalculated [See Fig. 2]. A separate set of parameters, c_{aD} and c_{rD} , were calculated in all cases for the deuteron-like nucleon interactions in triton, such that $E_D(r_D)=-2.2$ and $E_D'(r_D)=0$, when $r_D = 2.14$.

Fig. 2. Comparison of two nucleon (non-deuteron) interaction energies.

For Model A this yielded

$$E_\tau(r_\tau) = 2\left(\frac{c_a\, e^{-r_\tau \mu_a}}{r_\tau} + \frac{c_r\, e^{-r_\tau \mu_r}}{r_\tau}\right) + \left(\frac{c_{a_D}\, e^{-r_\tau \mu_a}}{r_\tau} + \frac{c_{r_D}\, e^{-r_\tau \mu_r}}{r_\tau}\right) + \left(\frac{3\hbar^2}{m{r_\tau}^2}\right) - \left(\frac{(4+{s_0}^2)\hbar^2}{m{r_\tau}^2}\right)$$

and for Model B this yielded

$$E_\tau(r_\tau) = \left(\frac{c_a\, e^{-r_\tau \mu_a}}{r_\tau} + \frac{c_r\, e^{-r_\tau \mu_r}}{r_\tau}\right) + \left(\frac{c_{a_D}\, e^{-r_\tau \mu_a}}{r_\tau} + \frac{c_{r_D}\, e^{-r_\tau \mu_r}}{r_\tau}\right) + \left(\frac{c_a\, e^{-\left(\frac{r_\tau}{2}\right)\mu_a}}{\left(\frac{r_\tau}{2}\right)} + \frac{c_r\, e^{-\left(\frac{r_\tau}{2}\right)\mu_r}}{\left(\frac{r_\tau}{2}\right)}\right) + \left(\frac{\hbar^2}{m{r_\tau}^2}\right) - \left(\frac{(4+{s_0}^2)\hbar^2}{3m{r_\tau}^2}\right)$$

Results

Results were obtained by setting the energy of triton to -8.48 MeV and varying radius of the two nucleon interaction (non-deuteron) to obtain a value close to 1.01 fm and a radius close to 1.94 fm [See Table 1].

Model A

Case	r_d	E_τ	r_τ	$r_\tau avg$	s_0
I	4.76	-8.48	3.34	1.93	1.01
II	4.79	-8.48	3.31	1.92	1.01
III	5.89	-8.48	3.17	1.83	1.01

Model B

Case	r_d	E_τ	r_τ	$r_\tau avg$	s_0
I	2.86	-8.48	2.47	2.06	1.02
II	2.88	-8.48	2.46	2.05	1.02
III	3.89	-8.48	2.29	1.91	1.02

Table 1. Results of triton Model A and B case I, II, and III. Energies are in MeV and radii are in fm.

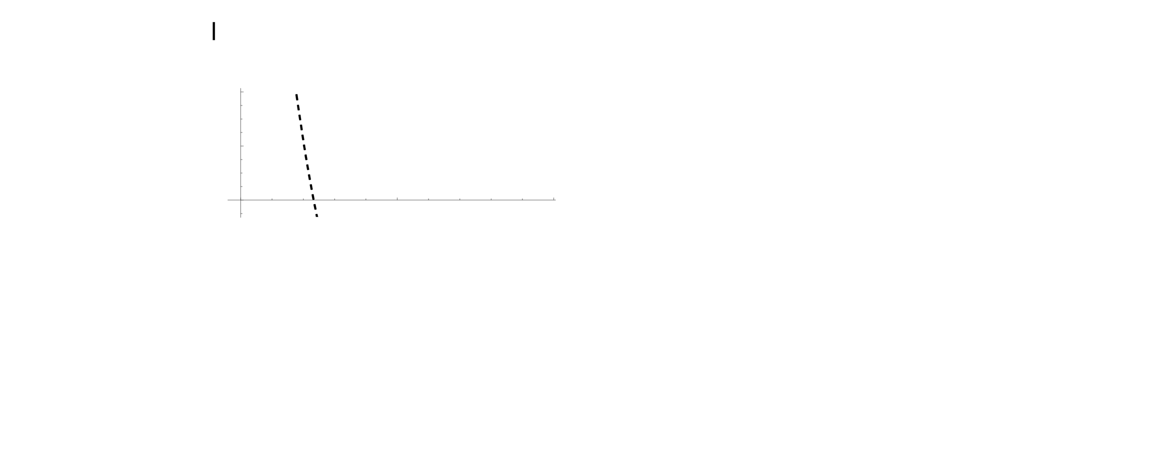

Fig. 3. Model A Case I energy curve. (Cases II and III are omitted since they are indistinguishable).

The results demonstrate that is possible to model small nuclei with a semi-classical model and the Efimov potential. Furthermore, the s_0 obtained from the results agrees with previous studies [5] and lends support to a universal value of 1.00624.

One failure of the Yukawa potential in our model is that for s_0 values larger than 0.785, $E_\tau \to -\infty$ as $r_\tau \to 0$. However, this is only a failure of the Yukawa potential since it dominates the energy equation at low r_τ due to its exponentials. This problem can be corrected with negligible impact on the energies of interest by multiplying the Efimov potential by $1\text{-}e^{-r_\tau \mu_b}$, or by simply using the Lennard-Jones potential.

Further investigation into the results reveals that as $r_{dmin} \to \infty$, the system reaches a steady state in agreement with the Virial Theorem.

Future research is needed to predict the locations of the Efimov states. Future research could also tweak the μ_a and μ_r pion interaction parameters to improve the results of geometric models A and B.

References

[1] V. Efimov, Phys. Lett. 33B (1970) 563.
[2] E. Braaten, H.-W. Hammer, Annals of Physics 322 (2007) 132.
[3] Y. Wang, J.P. D'Incao, C.H. Green, Phys. Rev. Lett. 106, 233201 (2011) 1.
[4] E. Braaten, H.-W. Hammer, Annals of Physics 322 (2007) 137.
[5] E. Braaten, H.-W. Hammer, Annals of Physics 322 (2007) 133.
[6] E. Braaten, H.-W. Hammer, Annals of Physics 322 (2007) 126.

Acknowledgements

Many thanks to Dr. Aldo Bonasera for his patience and mentorship, and to Dr. Sherry Yennello and the TAMU Cyclotron Institute for the opportunity to research here this summer. Funding was provided by an NSF grant.

Cyclotron Institute
Texas A&M University

National Science Foundation
WHERE DISCOVERIES BEGIN